03

Global-Scale Estimation of Diffuse Groundwater Recharge

Model Tuning to Local Data for Semi-Arid and Arid Regions and Assessment of Climate Change Impact

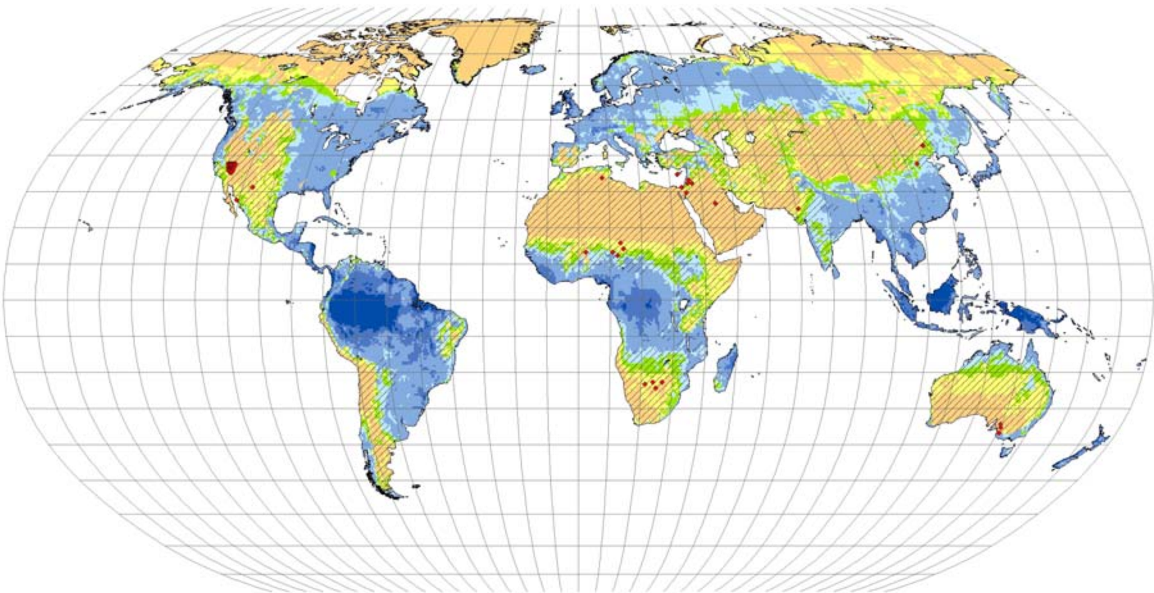

Petra Döll and Martina Flörke

August 2005

Frankfurt Hydrology Paper

JOHANN WOLFGANG GOETHE
UNIVERSITÄT
FRANKFURT AM MAIN

Global-Scale Estimation of Diffuse Groundwater Recharge

Model Tuning to Local Data for Semi-Arid and Arid Regions and Assessment of Climate Change Impact

Petra Döll
Institute of Physical Geography
Frankfurt University

Martina Flörke
Center for Environmental Systems Research
University of Kassel

August 2005

Frankfurt Hydrology Papers:

01 A Digital Global Map of Irrigated Areas – An Update for Asia
02 Global-Scale Modeling of Nitrogen Balances at the Soil Surface
03 Global-Scale Estimation of Diffuse Groundwater Recharge

Institute of Physical Geography, Frankfurt University
P.O. Box 11 19 32, D-60054 Frankfurt am Main, Germany
Phone +49 (0)69 798 22393, Fax +49 (0)69 798 25058
http://www.geo.uni-frankfurt.de/ipg/ag/dl/index.html

Please cite as:
Döll, P., Flörke, M. (2005): Global-Scale Estimation of Diffuse Groundwater Recharge. *Frankfurt Hydrology Paper 03*, Institute of Physical Geography, Frankfurt University, Frankfurt am Main, Germany.

Abstract

Groundwater recharge is the major limiting factor for the sustainable use of groundwater. To support water management in a globalized world, it is necessary to estimate, in a spatially resolved way, global-scale groundwater recharge. In this report, improved model estimates of diffuse groundwater recharge at the global-scale, with a spatial resolution of 0.5° by 0.5°, are presented. They are based on calculations of the global hydrological model WGHM (WaterGAP Global Hydrology Model) which, for semi-arid and arid areas of the globe, was tuned against independent point estimates of diffuse groundwater recharge. This has led to a decrease of estimated groundwater recharge under semi-arid and arid conditions as compared to the model results before tuning, and the new estimates are more similar to country level data on groundwater recharge. Using the improved model, the impact of climate change on groundwater recharge was simulated, applying two greenhouse gas emissions scenarios as interpreted by two different climate models.

Acknowledgments: The authors are grateful for the contribution of Mike Edmunds, University of Oxford, who compiled the estimates of local groundwater recharge in semi-arid and arid regions around the world. They thank Kerstin Schulze, University of Kassel, and Martin Hunger, Frankfurt University, for their programming work. Part of the research presented in this publication was funded by the International Atomic Energy Agency (IAEA), Vienna.

Table of Contents

1 Introduction

Groundwater recharge is the major limiting factor for the sustainable use of groundwater. To support water management in a globalized world, it is necessary to estimate, in a spatially resolved way, global-scale groundwater recharge. Therefore, L'vovich (1979) created a global map of groundwater recharge based on base flow analyses. Later, Döll et al. (2002) developed a global model of groundwater recharge as part of the global hydrological model WGHM (WaterGAP Global Hydrological Model, Döll et al., 2003; Alcamo et al., 2003). With a spatial resolution of 0.5 degree by 0.5 degree, WGHM first computes total runoff based on a time series of monthly climate variables (Mitchell et al., 2003) as well as soil and land cover characteristics. Groundwater recharge is then calculated as a fraction of total runoff using data on relief, soil texture, geology and permafrost/glaciers. WGHM is tuned against measured river discharge only but not against independent estimates of (local-scale) groundwater recharge. Please note that here the term groundwater recharge refers only to diffuse recharge from the soil to the groundwater; groundwater recharge from rivers or other surface waters is not taken into account.

One difficulty of modeling groundwater recharge with a macro-scale hydrological model is that different from river discharge, no direct measurements of groundwater recharge are available. Besides, river discharge integrates over the whole drainage basin, while groundwater recharge estimates are generally rather local. Baseflow analysis of river hydrographs is generally considered to provide an integral estimate of groundwater recharge, but results are very dependent on the applied analysis method (Bullock et al., 1997; Tallaksen, 1993), and it cannot be done for river gauging stations downstream of large reservoirs, lakes or wetlands upstream (L'vovich, 1979). Besides, groundwater recharge is likely to be larger than the baseflow observed at a downstream location, in particular in arid and semiarid regions, where groundwater recharge might evapotranspirate at some location upstream of the gauging station (Margat, 1990). Finally, it must be kept in mind that the concept of renewable groundwater resources and its relation to groundwater recharge and base flow is scale-dependent as a part of the groundwater recharge might reappear as surface water after a very short travel distance.

Unfortunately, there are no reliable estimates of groundwater recharge at the country scale. In the compilation of country values of groundwater recharge (WRI, 2000), many values stem from Margat (1990) which again often used estimates of the global-scale baseflow analysis of L'vovich (1979).

For semi-arid and arid conditions, modeling of runoff and groundwater recharge is generally found to be more difficult than in humid areas, mainly due to the small values of the variables of interest. However, for these climatic conditions, it is possible to estimate local-scale groundwater recharge based on the analysis of chloride profiles in the soil and isotope measurements. These estimates provide a unique opportunity to increase the capacity of WGHM to reliably estimate groundwater recharge in semi-arid and arid regions.

Here, we present a method for tuning the groundwater module of WGHM against independent local-scale estimates of groundwater recharge in semi-arid and arid regions. The goal is to obtain improved estimates of groundwater recharge for semi-arid and arid regions. As a result of the analysis of the independent estimates and of the relation between those values and the model output (section 3), the WGHM algorithm to compute groundwater recharge, which is described in section 2, is modified for semi-arid and arid grid cells. The new groundwater recharge estimates are then combined with the existing groundwater recharge estimates of WGHM for humid areas to generate a global map of groundwater recharge that contributes to the international WHYMAP (**W**orld-wide **Hy**drogeological **M**apping and **A**ssessment **P**rogramme) effort (http://www.bgr.de/b1hydro/index.html?/b1hydro/fachbeitraege/a200401/e_whymap.htm). In section 4, the new global map of diffuse groundwater recharge during the climate normal 1961-90 is presented and the map quality is discussed. Besides, using the improved groundwater recharge algorithm, the impact of climate change on groundwater recharge is assessed in section 5. Finally, conclusions are drawn (section 6).

2 Method to compute groundwater recharge in the standard version of WGHM

In order to calculate groundwater recharge in WGHM, total runoff from the land area of each cell is partitioned into fast (surface and sub-surface) runoff and groundwater recharge. This is done following a heuristic approach which is based on qualitative knowledge about the influence of certain characteristics (for which global data sets are available) on the partitioning of total runoff: slope characteristics (Günther Fischer, IIASA, personal communication, 1999), soil texture (FAO, 1995), hydrogeology (Canadian Geological Survey, 1995) and the occurrence of permafrost and glaciers (Brown et al., 1998; Hoelzle and Haeberli, 1999). Land cover characteristics are not included; in their study on base flow indices in the Elbe river basin, Haberlandt et al. (2001) found that the proportion of forest and arable land in sub-basins of or below the size of 0.5° grid cells only had a weak influence on the baseflow index (baseflow as a ratio of total runoff).

In the standard version of WGHM, groundwater recharge R_g is computed for all grid cells and with a daily time step as

$$R_g = \min(R_{g\max}, f_g R_l) \quad \text{with} \quad f_g = f_r\, f_t\, f_a\, f_{pg} \tag{1}$$

R_{gmax} = soil texture specific maximum groundwater recharge [mm/d]
R_l = total runoff of land area [mm/d]
f_g = groundwater recharge factor ($0 \le f_g < 1$)
f_r = relief-related factor ($0 < f_s < 1$)
f_t = texture-related factor ($0 \le f_t \le 1$)
f_a = aquifer-related factor ($0 < f_a < 1$)
f_{pg} = permafrost/glacier-related factor ($0 \le f_g \le 1$)

The cell-specific values of all four factors and of the texture specific maximum groundwater recharge are defined by 1) assigning values to property classes of the global data sets and 2) upscaling to 0.5° x 0.5°. Appendix A provides a description of the factors and data sets. Groundwater recharge from surface water bodies (lakes, wetlands and rivers) is not taken into account.

3 Tuning of the groundwater recharge model of WGHM

The groundwater recharge model of WGHM was only tuned for semi-arid and arid grid cells, i.e. those with long-term average (1961-90) precipitation less or equal to half the potential evapotranspiration. The grid cells which obey this rule but are north of 60°N were excluded (see Fig. 1 for the extent of semi-arid and arid regions in WGHM). In the following, the term "semi-arid" is used instead of "semi-arid and arid".

The model was tuned against 25 estimates of groundwater recharge world-wide derived from chloride profiles and isotope data (compiled by Mike Edmunds, University of Oxford, personal communication, 2003). They are from measurements in Northern and Southern Africa, the Near East, Asia and Australia (Fig. 1). These estimates are thought to be representative not only for a measurement point but a larger area. In most cases, the data are representative for the 50-100 year period before the measurements. In addition, groundwater recharge computed by a meso-scale hydrological model of the Death Valley region in south western USA (Hevesi et al., 2003) was upscaled to derive estimates for the 26 0.5° grid cells of WGHM which cover the region (Fig. 1). These model results are representative for the time period 1950-1999.

A comparison of the long-term average (1961-90) groundwater recharge values as computed by the standard ("untuned") WGHM version 2.1e showed that the model overestimates all groundwater recharge values below 10 mm/a (Fig. 2). The long-term average is the mean of daily groundwater recharge calculated for the time period 1961-90. Please note that the daily precipitation values applied in WGHM are no measured daily precipitation values as only 0.5 degree gridded monthly precipitation is available at the global scale. Information on the number of wet days per month is used to determine a sequence of dry and wet days, and the monthly precipitation sum is equally distributed to the wet days such that all wet days of a month have the same precipitation value (climate information is taken from Mitchell et al., 2003). Tuning was aimed at minimizing the discrepancies between model results and independent estimates by adjusting the groundwater recharge algorithm in an globally homogeneous way, i.e. without site- or region-specific adjustments (given the few independent estimates).

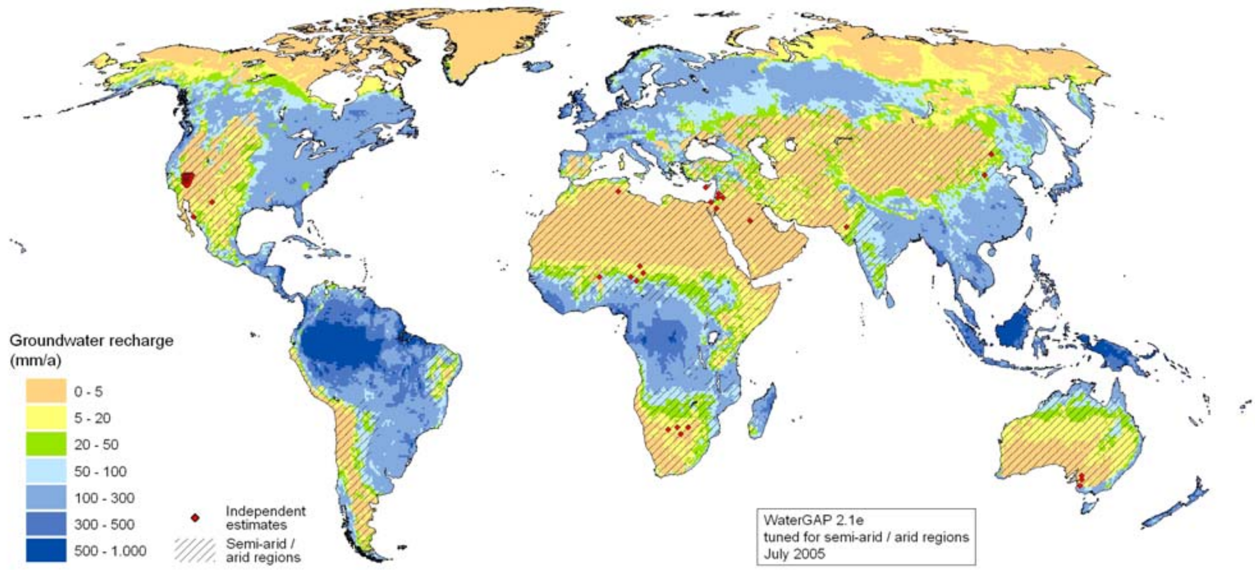

Fig. 1: Long-term average groundwater recharge for the period 1961-90 as computed by the tuned version of WHGM 2.1e [mm/a]. The semi-arid and arid regions for which tuning has been performed are indicated, as well as the locations of the independent estimates of groundwater recharge against which the model has been tuned.

There could be two reasons for the overestimation of very low groundwater recharge values:

1. Total runoff is overestimated
2. Groundwater recharge as a fraction of total runoff is overestimated

If reason 1 were true, the computation of total runoff in WHGM should be modified, not only the partitioning of total runoff into fast surface/subsurface flow and groundwater recharge. We suspect that WGHM tends to overestimate groundwater recharge under semi-arid conditions as in many semi-arid river basins we need to decrease total runoff to match long-term average observed river discharge (Döll et al., 2003). In semi-arid basins without discharge measurements, overestimation of total runoff is likely. The overestimation might be due to, among other reasons, surface/subsurface runoff and also groundwater recharge flowing into small ephemeral ponds from which most of the local-scale runoff then evapotranspirates. For the Death Valley region, WGHM appears to overestimate total runoff by about an order of 10 (50 mm/a instead of 5 mm/a), which can only partially be explained by precipitation. Precipitation is higher in the climate data set applied in WGHM than in the meso-scale model of Hevesi et al. (2003) (207 mm/a vs. 174 mm/a).

If reason 2 were true, the preferred tuning method would be to modify the groundwater recharge factors f_r, f_t and f_a, as well as R_{gmax}, which depend on the relief, texture and hydrogeology of the grid cell. However, the analysis of these characteristics for the 51 grid cells with independent estimates showed that an adjustment of the recharge factors would not lead to the necessary changes in groundwater recharge, in particular in cells with a strong

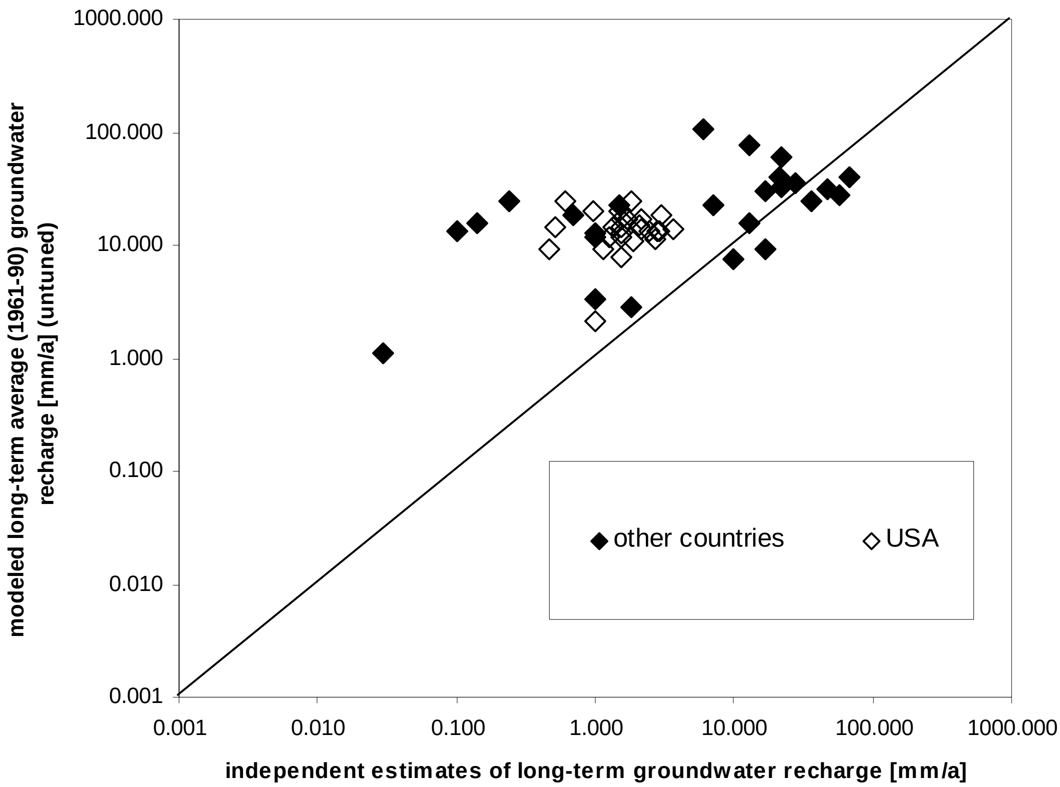

Fig. 2: Comparison of long-term average (1961-90) groundwater recharge as computed by the standard version of WGHM with independent estimates for 51 grid cells.

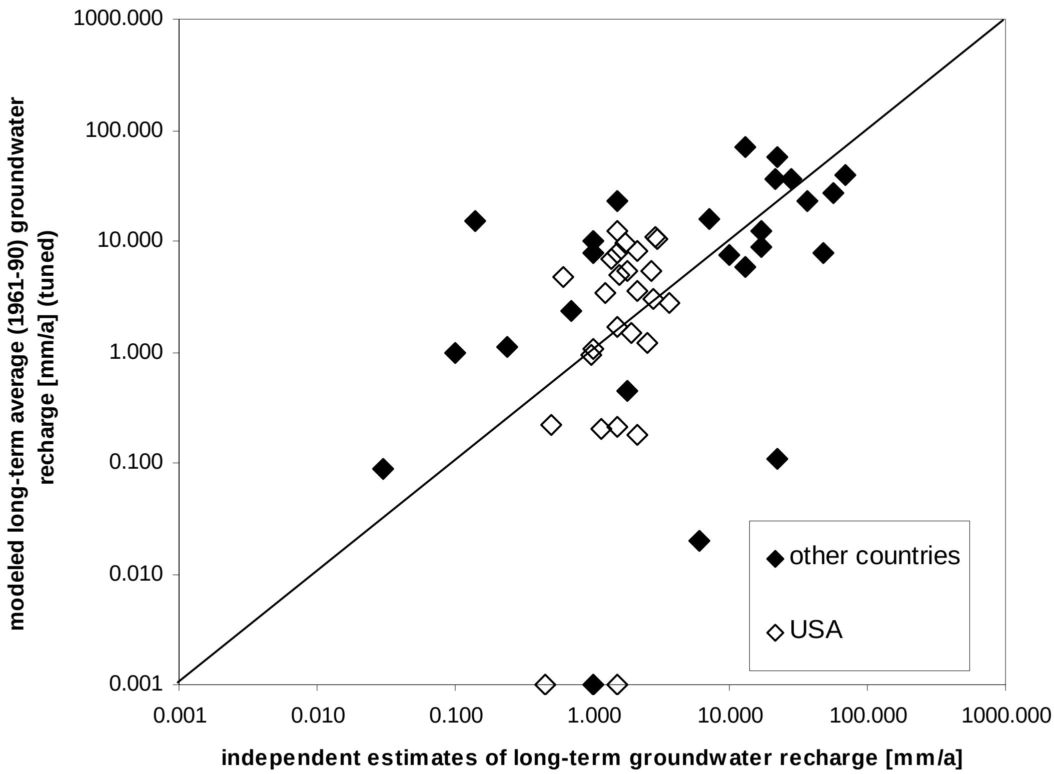

Fig. 3: Comparison of long-term average (1961-90) groundwater recharge as computed by the tuned version of WGHM with independent estimates for 51 grid cells.

overestimation of recharge. In many of these cells, relief, texture and hydrogeology is such that groundwater recharge should be a large fraction of total runoff (flat terrain, coarse soil texture and young sedimentary aquifers), according to the heuristic relations implemented in WGHM (Tables A1, A2 and A3 in the appendix).

Let us now analyze the differences of runoff and groundwater recharge processes between semi-arid and humid climate conditions, as the standard version of WGHM, like most hydrological models, appears to better represent humid conditions than semi-arid conditions. Compared to humid regions, semi-arid regions are characterized by the following characteristics.

- A larger variability of precipitation with more heavy rainfalls.
- Surficial crusting in areas of weak vegetation cover, which strongly reduces infiltration into the soil.
- Reduced infiltration of heavy rain into dry soil due to pore air which has to be released first to allow the infiltration.
- More infiltration and thus groundwater recharge in soils with fine texture as compared to soils with coarse texture. The low unsaturated hydraulic conductivity of dry sands, for example, leads to a lower infiltration capacity for sand as compared to loam, which, at the same matric potential, has a much higher water content and unsaturated hydraulic conductivity. Under humid, i.e. wetter conditions, the unsaturated hydraulic conductivity of sand and thus groundwater recharge is generally higher than that of loam.
- In some regions, e.g. Namibia, groundwater recharge only occurs via fissures in crystalline rock which allow the rainwater to leave the zone of capillary rise faster in the case of sand. Rainwater that remains in the capillary zone evaporates due to high temperatures and radiation in semi-arid regions. In humid regions, groundwater recharge is fissured crystalline rocks is expected to be lower than in sandy sediments.

Altogether, in semi-arid regions groundwater recharge appears to be confined to periods of exceptionally heavy rainfall (Vogel and Van Urk, 1975), in particular if soil texture is coarse.

We conclude that WGHM is likely to overestimate groundwater recharge in many semi-arid regions due to an overestimation of both total runoff and the fraction of groundwater recharge. As a modification of the computation of total runoff is beyond the scope of this research, and a simple adjustment of the recharge factors is not effective, we chose to derive an add-on reduction algorithm for groundwater recharge in semi-arid areas which leads to improved estimates of groundwater recharge. These estimates are a valuable end product, but they are not yet consistently implemented in WGHM. Considering the specific circumstances and the computation of processes in semi-arid regions listed above, the daily groundwater recharge R_g is set to zero on days without heavy rain, if the soil texture of a semi-arid grid cell is medium to coarse:

$R_g = 0$ if $P \leq 10$ mm/d (and grid cell is semi-arid and soil texture is medium to coarse)

Medium to coarse soil texture refers to an average grid cell texture value of less than 21 (compare Table A2 in the Appendix). 46 out of the 51 grid cells with independent estimates of groundwater recharge fulfill this condition, such that their groundwater recharge is modified. Four out of the five grid cells with fine to medium soil texture, which also have relatively independent recharge values of 10-70 mm/a, are subject to an underestimation of groundwater recharge already with the standard version of WGHM. The algorithm was designed in a trial-and-error procedure, in which computed groundwater recharge values and independent estimates were compared for all 51 grid cells.

4 Groundwater recharge under current climate and discussion of model quality

Fig. 3 shows that after tuning, the computed recharge values for the 51 grid cells are no longer biased towards high values. The average groundwater recharge for Death Valley region (USA), for example, decreased from 14 to 4 mm/a, compared to the average of the independent values of 2 mm/a. The modeling efficiency for all cells increased from -0.41 to +0.05. For two cells in Australia, with independent estimates of 6 and 22 mm/a, however, the new algorithm leads to a significant underestimation of recharge, while the Damascus (Syria) grid cell is still overestimated considerably (22 mm/a instead of 1.5 mm/a) because the reduction algorithm is not applied due to the fine texture of the soil.

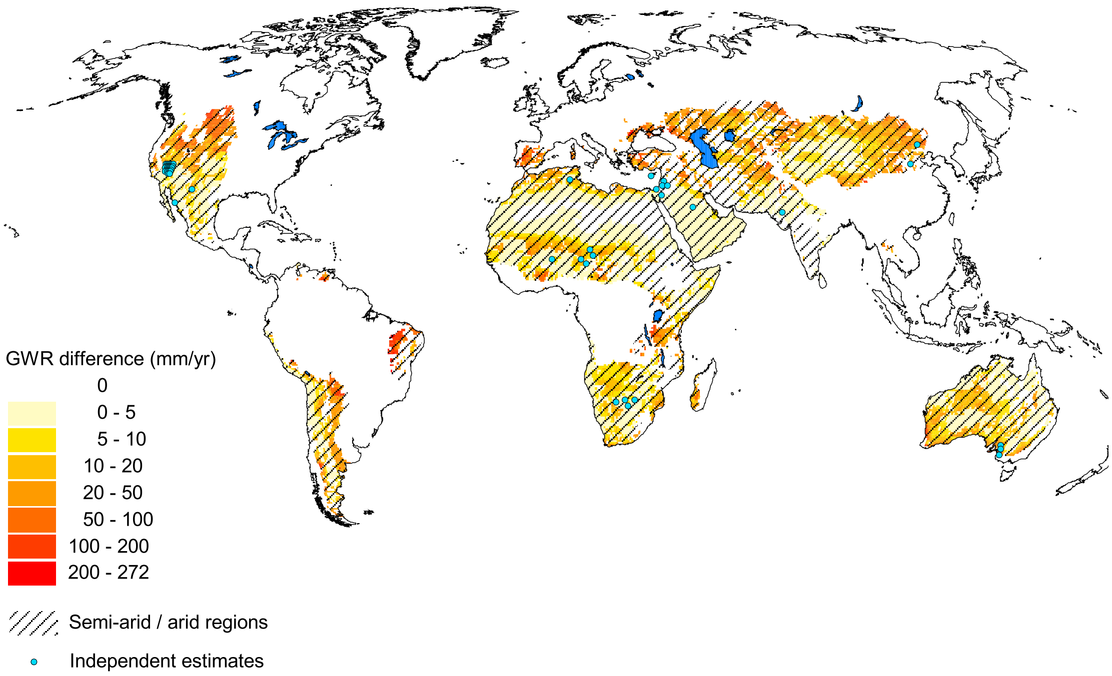

Fig. 4: Reduction of estimated groundwater recharge by model tuning: Difference between standard and tuned long-term average (1961-90) groundwater recharge [mm/a]. The stippled white areas are those semi-arid and arid regions where model tuning did not result in a reduction of groundwater recharge.

Due to the lack of information, it is difficult to judge the plausibility of the computed estimates of groundwater recharge. After tuning, there are large regions of the globe with less than 2 mm/a of groundwater recharge. Where the reduction due to tuning is high, either the new estimates are too low, or groundwater recharge and runoff in the standard version are too high. The latter seems to be true in Northeastern Brazil, for example, while the former may be true at the northern coast of the Black Sea.

A weak type of model validation is the comparison of computed country values of groundwater recharge to the rather uncertain values provided by WRI (2000). Fig. 5 presents a global map of average country values of computed groundwater recharge, while Fig. 6 shows the comparison to WRI data. We defined countries to be “semi-arid” if more than 34% of the country’s cells are defined as semi-arid in this investigation (which makes the USA a semi-arid country). The bias towards high groundwater recharge in semi-arid countries is almost eliminated, and the modeling efficiency for semi-arid countries improves from 0.14 to 0.18 for recharge in mm/a (and from 0.87 to 0.89 for recharge in km^3/a). Tuning reduces the total groundwater recharge in semi-arid countries that are included in the WRI data set from 3698 to 3279 km^3/a, as compared to 3205 km^3/a according to WRI (2000). For the remaining humid countries, modeling efficiency remains at 0.43 for recharge in mm/a (0.81 for recharge in km^3/a), whereas the overall modeling efficiency for all countries remains at 0.58 (0.84 for recharge in km^3/a). Total groundwater recharge in humid countries included in the WRI data set (not considering Yugoslavia) decreases from 8978 to 8885 km^3/a, as compared to 7646 km^3/a according to WRI (2000) (WGHM computes lower values in particular for Brazil, Canada, Indonesia and Russia). Total global groundwater recharge is computed to be 12882 km^3/a, as compared to 13442 km^3/a without tuning. This global value is 12% larger than the value estimated by L'vovich (1979) by a global-scale baseflow analysis for almost 1500 rivers (800 of them in the former Soviet Union), which certainly is still the best continental or global scale analysis that exists up to today. However, no discharge data had been available for 80% of South America, 20% of Africa (not counting the Sahara and the Kalahari), 60% of Australia (not counting the desert), and some parts of Asia and Canada.

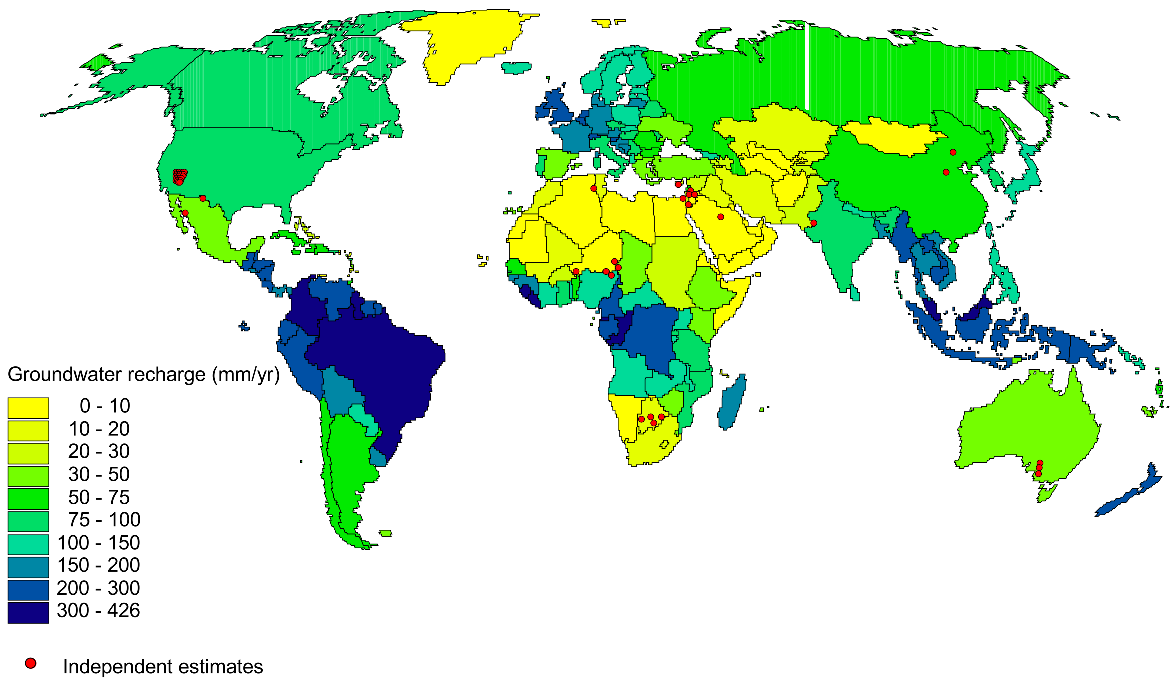

Fig. 5: Country averages of long-term average (1961-90) groundwater recharge as computed by the tuned WGHM 2.1e [mm/a].

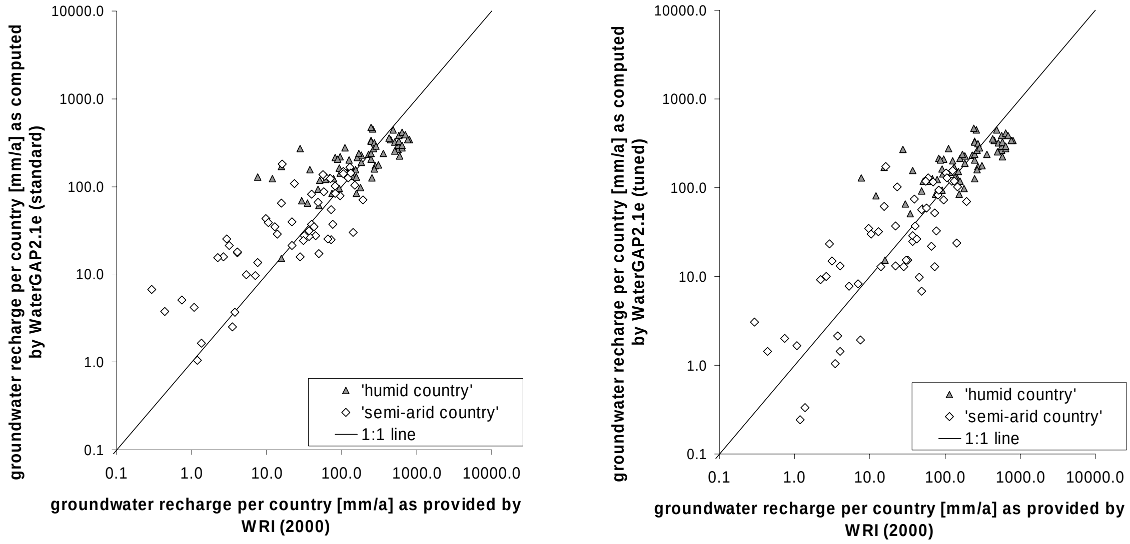

Fig. 6: Comparison of average groundwater recharge per country [mm/a] between standard (left) and tuned (right) version and independent data of WRI (2000).

5 Impact of climate change on groundwater recharge

Due to anthropogenic climatic change, groundwater recharge is and will be changing as both the total runoff and the partitioning of total runoff into surface and fast subsurface flow and groundwater recharge is altered. Everywhere, increased temperature will increase potential evapotranspiration, which decreases total runoff. However, total runoff as well as groundwater recharge will mainly change with the change in precipitation. Here, precipitation change during the major recharge season is most relevant. In temperate climates, an increase in precipitation is generally foreseen during the winter season where most recharge occurs. However, the recharge period might be shortened as during the hotter summers, there is increased evapotranspiration in particular if the groundwater table is close to the land surface. Using a coupled groundwater and soil model for a groundwater basin in Belgium, Brouyère et al. (2004) computed a decrease of groundwater recharge for climate scenarios of three different climate models which predict less summer and more winter precipitation.

The impact of increased temporal variability of precipitation on groundwater is site-dependent. More heavy rains can lead to more groundwater recharge in particular in semi-arid areas where macropores and joints often function as fast conduits for water down to soil depths and evapotranspiration becomes ineffective. However, increased temporal variability of precipitation is also likely to lead to soil crusting and hydrophobe soils, such that overland flow increases and groundwater recharge decreases. If heavy rain falls on already wet soil, the additional precipitation cannot infiltrate and becomes excess saturation overland flow.

Less groundwater recharge leads to a decrease of the safe basin yield, i.e. it might require decreased groundwater withdrawals. It leads to a drop in the groundwater table, which can have a negative impact on vegetation. Increased groundwater recharge might be problematic, too, e.g. for vegetation used to a lower water table, or in built-up areas. How a change of groundwater recharge is translated into a change in groundwater table or level is site-specific.

5.1 Climate change scenarios

In this study, four different climate change scenarios were taken into account, looking at the situation in the 2050s. The two IPCC greenhouse gas emissions scenarios A2 and B2 (Nakicenovic and Swart, 2000) as translated into climate change scenarios by two state-of-the-art global climate models, the ECHAM4/OPYC3 model (Röckner et al., 1996, hereafter referred to as ECHAM4) and the HadCM3 model (Gordon et al., 1999) result in four different climate change scenarios (data available at the IPCC Data Distribution Center, http://ipcc-ddc.cru.uea.ac.uk/). In the A2 scenario, emissions increase from 11 Gt C/a (CO_2-equivalent) in 1990 to 25 Gt C/a in the 2050s, but only to 16 Gt C/a in the case of scenario B2. Due to climate model uncertainties, the same emissions scenarios are translated to rather different climate scenarios, in particular with respect to precipitation.

The changes in averages of monthly precipitation and climate values between the periods 1961-1990 and 2041-2070 as computed by the climate models were used to scale the grid cell values of observed monthly precipitation and temperature between 1961 and 1990 that are generally used to drive WGHM. In a first step, the climate model data were interpolated from their original resolutions to the WGHM resolution of 0.5° by a simple interpolation procedure. Then, in the case of temperature, the observed values are scaled by adding to them the difference of the climate model values of future (2041-2070) and present-day (1961-1990) temperature, while the 30-year perturbed precipitation time series was produced by multiplying the observed values with the future climate model precipitation as a ratio of the present-day precipitation. If the present-day monthly precipitation is less than 1 mm, precipitation is scaled additively, like temperature. Until now, global climate models cannot reproduce well observed climate variability, and therefore they do not reliably simulate future climate variability, either. However, they do simulate a general increase in climate variability.

5.2 Changes in groundwater recharge

Fig. 7 shows the changes of long-term average annual diffuse groundwater recharge by the 2050s as compared to the climate normal 1961-1990. The overall pattern of change is rather similar in all four scenarios. In each scenario, Northeastern Brazil, the western part of southern Africa and the areas along the southern rim of the Mediterranean Sea may suffer from very strong decreases of groundwater recharge of more than 70%. Other areas that will suffer from strong to very strong decreases are climate model dependent (e.g. within Australia, the USA or Spain). In large areas of the globe, groundwater recharge may increase by more than 30%, in particular in the Sahel, the Near East, Northern China, Western US and Siberia. To assess the impact of climate, please take into account the (often very low) current values of groundwater recharge in Fig. 7.

The very large emissions differences between A2 and B2 do not lead to very different changes in groundwater recharge, and at least for some regions (e.g. Australia and India) the difference between the results of the two climate models for the same emissions scenario are more significant than the differences between the two emissions scenarios as interpreted by any one climate model. Thus, groundwater recharge cannot be used as a variable that can serve as a guideline for emissions reductions.

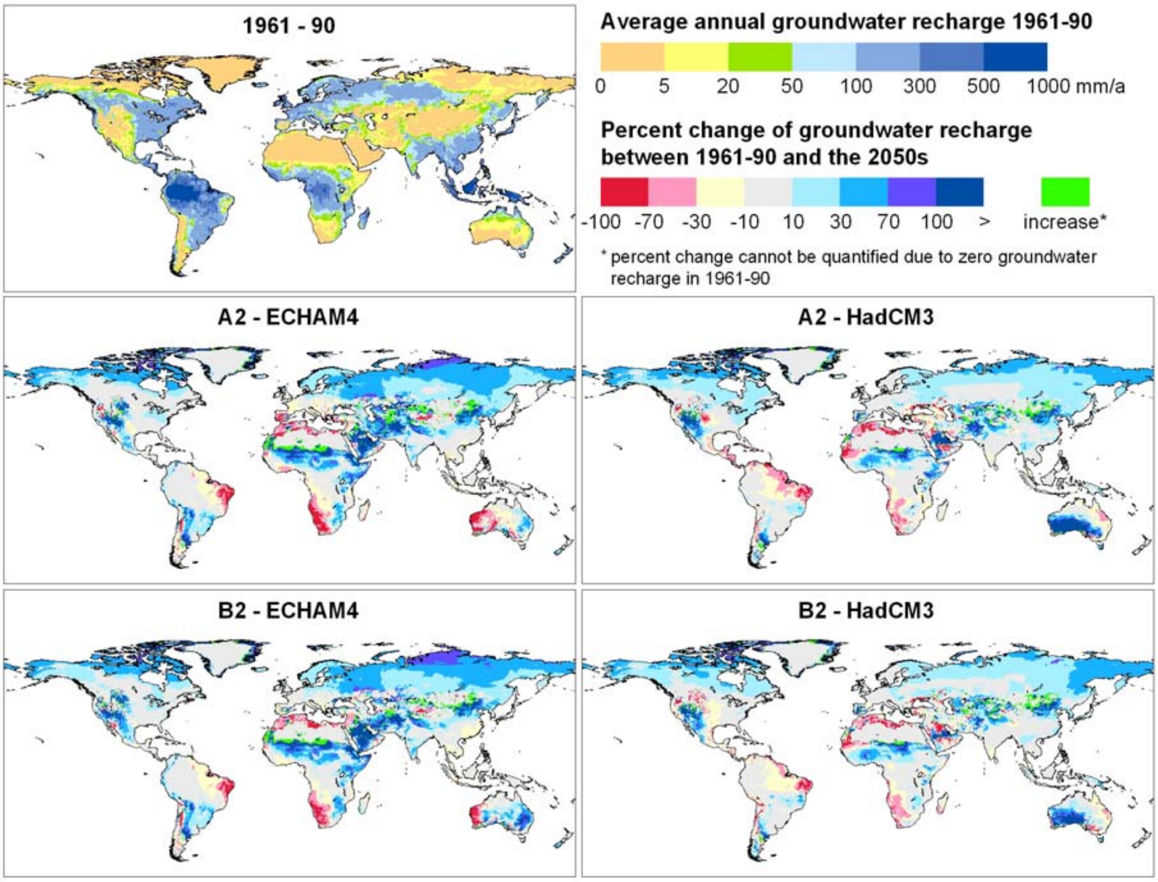

Fig. 7: Impact of climate change on long-term average annual diffuse groundwater recharge. Percent changes of 30-year averages groundwater recharge between 1961-1990 and the 2050s (2041-2070), as computed by WGHM applying four different climate change scenarios (climate scenarios computed by the climate models ECHAM4 and HadCM3, each iterpreting the two IPCC greenhouse gas emissions scenarios A2 and B2).

A comparison of the impact of climate change on groundwater recharge to the impact on total runoff generation from the land fraction of each cell (i.e. not considering the water balance of surface water bodies) shows a spatially very heterogeneous pattern, even though groundwater recharge, in WGHM, is computed as a fraction of total runoff from land (compare Eq. 1). In most areas, however, the percent change in groundwater recharge is less than the percent change in total runoff generation from land. In the monsoonal regions of Asia as well as in most humid areas of South America, the percent increase in groundwater recharge is much lower than the percent change in total runoff from land, as the infiltration capacity of the soil R_{gmax} (Eq. 1) limits any additional runoff in becoming groundwater recharge. In other humid areas e.g. in Poland and Russia, a seasonal shift of precipitation and evapotranspiration causes a relatively stronger increase of groundwater recharge because under future climate, the infiltration capacity limits recharge during less days than under current climate even if total annual runoff is increased. In some areas around the globe, (mostly small) increases of total runoff from land are coupled to (mostly small) decreases in groundwater recharge, and vice versa, which is also due to seasonal shifts. In areas with decreasing total runoff from land, the percent decrease of groundwater recharge is often higher than the percent decrease of total runoff from land, which appears to be partially due to the assumption that groundwater recharge in semi-arid areas only occurs if daily precipitation is larger than 10 cm. Please not that the described pattern of change does not follow the outline of semi-arid regions even though there are different model algorithms for humid and semiarid areas. However, those semi-arid areas that suffer from very strong decreases of groundwater recharge (Northeastern Brazil, the western part of southern Africa and the areas along the southern rim of the Mediterranean Sea), the groundwater change signal is generally stronger than the total runoff signal.

Table 1 shows the simulated changes of the global values of groundwater recharge, total runoff from land and total cell runoff (which includes evaporation from lakes and wetlands as well as evaporation of the water that is withdrawn for human water use). While both runoff values increase by approximately 9% between 1961-1990 and the 2050s (in the case of the ECHAM4 A2 scenario, with an increase of continental precipitation of 4%), groundwater recharge increases by only 2%. The effect of neglecting increased future climate variability on groundwater recharge as computed by WGHM cannot be estimated without actual computations of groundwater recharge under the impact of changed climate variability, as the effect is expected to be both cell-specific and depending on the precise change of climate variability.

Table 1: Global values of groundwater recharge, total runoff from land, total cell runoff and continental precipitation computed or applied by WGHM for the period 1961-1990 and the 2050s. The values for the future time period refer to the emissions scenario A2 as interpreted by the global climate model ECHAM4.

	1961-1990 (A) [km^3/a]	2050s (ECHAM4, A2) (B) [km^3/a]	Change between A and B [%]
Groundwater recharge	12882	13112	+1.8
Total runoff from land	38617	42062	+8.9
Total cell runoff [1]	36621	39755	+8.6
Continental precipitation	107047	111572	+4.2

[1] including the water balance of lakes and wetlands and the evapotranspiration of withdrawn water (assumed to remain unchanged), and equivalent to the renewable water resources

6 Conclusions

A comparison of groundwater recharge as computed by the standard version of WGHM to independent estimates of groundwater recharge at 25 locations world-wide as well as to the results of a meso-scale hydrological model for the Death Valley region in the USA showed that long-term average groundwater recharge below 10 mm/a is strongly overestimated by WGHM in most cases. Tuning of the groundwater recharge module of the global hydrological model WGHM for semi-arid and arid regions of the globe resulted in decreased values of groundwater recharge which seem to represent actual groundwater recharge somewhat better. At least, the significant bias towards high values of groundwater recharge in semi-arid and arid areas has been removed. However, uncertainty remains high.

The produced global map of long-term average groundwater recharge is unique in that it combines state-of-the-art global scale hydrological modeling with independent information on local-scale groundwater recharge in semi-arid and arid areas. The predictive capacity of WGHM for semi-arid and arid conditions has been improved by taking advantage of local-scale information on groundwater recharge that is available in semi-arid and arid regions only. Further validation and improvement of the WGHM groundwater recharge model requires more independent local-scale estimates of groundwater recharge. Modeling of total runoff from land and evapotranspiration in semi-arid and arid areas will be improved by taking into account the independent local-scale estimates of groundwater collected for this study.

Under the impact of climate change, groundwater recharge will increase in the largest part of the globe by the 2050s, but mostly not as much as total runoff because recharge capacity is limited. In some semi-arid areas, in particular in Northeastern Brazil, the western part of southern Africa and the areas along the southern rim of the Mediterranean Sea, groundwater recharge will decrease very strongly, according to the four climate scenarios applied. In the future, we plan to improve the assessment of climate change impacts on groundwater recharge by taking into account climate variability changes.

7 References

Alcamo, J., Döll, P., Henrichs, T., Kaspar, F., Lehner, B., Rösch, T., Siebert, S. (2003): Development and testing of the WaterGAP 2 global model of water use and availability. Hydrological Sciences. 48 (3), 317-337.

Brouyère, S., Carabin, Dassargues, A. (2004): Climate change impacts on groundwater resources: modelled deficits in a chalky aquifer, Geer basin, Belgium. Hydrogeology Journal, 12, 123-134.

Brown, J., Ferrians, O.J. Jr., Heginbottom, J.A., Melnikov, E.S. (1998): Digital Circum-Arctic Map of Permafrost and Ground-Ice Conditions. International Permafrost Association Data and Information Working Group, Circumpolar Active-Layer Permafrost System

(CAPS), CD-ROM version 1.0. National Snow and Ice Data Center, University of Colorado, Boulder, Colorado.

Bullock, A., Andrew, A., Mngodo, R. (1997): Regional surface water resources and drought assessment. In: Southern African FRIEND, Technical Documents in Hydrology No. 15, UNESCO, Paris, 40-93.

Canadian Geological Survey (1995): Generalized Geological Map of the World and Linked Databases. Open File Report 2915d. CD-ROM.

Döll, P., Kaspar, F., Lehner, B. (2003): A global hydrological model for deriving water availability indicators: model tuning and validation. Journal of Hydrology, 270 (1-2), 105-134.

Döll, P., Lehner, B., Kaspar, F. (2002): Global modeling of groundwater recharge. In Schmitz, G.H. (ed.): Proceedings of Third International Conference on Water Resources and the Environment Research, Technical University of Dresden, Germany, Vol. I, 27-31.

FAO (1995): Digital Soil Map of the World and Derived Soil Properties. CD-ROM version 3.5.

Gordon, C., Cooper, C., Senior, C.A., Banks, H., Gregory, J.M., Johns, T.C., Mitchell, J.F.B., Wood, R.A. (2000): The simulation of SST, sea ice extents and ocean heat transports in a version of the Hadley Centre coupled model without flux adjustments, Climate Dynamics 16 (2/3), 147-168.

Haberlandt, U., Klöcking, B., Krysanove, V., Becker, A. (2001): Regionalisation of the base flow index from dynamically simulated flow components – a case study in the Elbe River Basin. Journal of Hydrology, 248, 35-53.

Hevesi, J.A., Flint, A.L., Flint, L.E. (2003): Simulation of Net Infiltration and Potential Recharge Using a Distributed-Parameter Watershed Model of the Death Valley Region, Nevada and California. USGS Water-Resources Investigations Report 03-4090. USGS, Sacramento, USA. (http://water.usgs.gov/pubs/wri/wri034090/, 13.09.04)

Hoelzle, M., Haeberli, W. (1999): World Glacier Inventory. World Glacier Monitoring Service. National Snow and Ice Data Center. University of Colorado, Boulder, Colorado.

L'vovich, M.I. (1979): World Water Resources and their Future. American Geophysical Union.

Margat, J. (1990): Les Eaux Souterraines dans le Monde. BRGM R31780, Orleans, France.

Mitchell, T.D., Carter, T.R., Jones, P.D., Hulme, M., New, M. (2003): A comprehensive set of high-resolution grids of monthly climate for Europe and the globe: the observed record (1901-2000) and 16 scenarios (2001-2100). Journal of Climate: submitted.

Nakicenovic, N., Swart, R. (eds.) (2000): Emission Scenarios. IPCC Special Report on Emission Scenarios. Cambridge University Press. (http://www.ipcc.ch)

Röckner, E., Arpe, K., Bengtsson, L., Christoph, M., Claussen, M., Dümenil, L., Esch, M., Giorgetta, M., Schlese, U., Schulzweida, U. (1996): The atmospheric general circulation model ECHAM-4: Model description and simulation of present day climate, MPI-Report No. 218, MPI für Meteorologie, Hamburg.

Tallaksen, L.M. (1995): A review of baseflow recession analysis. Journal of Hydrology, 165, 249-270.

Vogel, J.C., Van Urk, H. (1975): Isotopic composition of groundwater in semi-arid regions of southern Africa. J. Hydrol., 25, 23-26.

WRI (2000): World Resources 2000-2001.

Appendix

Description of factors in the groundwater recharge model of WGHM

Relief

Based on the GTOPO30 DEM with a resolution of around 1 km (USGS EROS data center), IIASA produced a map of slope classes with a resolution of 5 min (data provided by Günther Fischer, February 1999) which includes the fraction of each cell that is covered by a certain slope class. Seven slope classes are distinguished (Table A1). The 5-min-map was aggregated and mapped onto the 0.5° x 0.5° land mask, such that the percentage of each slope class with respect to the total land area of each 0.5° cell is produced. An "average relief" s_{avg} , ranging from 10 to 70, is computed as

$$s_{avg} = \sum_{i=1}^{7} slope\ class_i * 10 * frac_i$$

$frac_i$ = areal fraction of slope class i within the 0.5° cell

The relief-related groundwater recharge factor f_r for each slope class is given in Table A1. For each cell with an average relief s_{avg}, the respective value for f_r is obtained by linear interpolation.

Table A1: Slope classes and the relief-related groundwater recharge factor.

slope class	slope [%]	relief	f_r
1	0-2	10	1
2	2-5	20	0.95
3	5-8	30	0.90
4	8-16	40	0.75
5	16-30	50	0.60
6	30-45	60	0.30
7	<45	70	0.15

Texture

Soil texture is derived from the FAO Digital Soil Map of the World and Derived Soil Properties (FAO, 1995). The digital map shows, for each 5' by 5' raster cell, the soil mapping unit. For each of the 4931 soil mapping units, the following information is provided:

- names of up to 8 soil units that constitute the soil mapping unit
- the area of each soil unit in percent of the total area of the soil mapping unit
- the area of each soil unit belonging to one of three texture classes and to one of three slope classes

The soil texture provided by FAO is only representative for the uppermost 30 cm of the soil.

We assigned a texture value of 10 to coarse texture, a value of 20 to medium and a value of 30 to fine texture (Table A2). Based on the FAO information, an areally weighted average texture value was computed for the 5' cells, which was then averaged for land area of each 0.5° cell.

For the following soil units, texture was not given: dunes, glacier, bare rock, water, and salt. The texture value of dunes was set to 10. All other four soil unit types were not taken into account for computing the areal averages (the bare rock extent in the FAO data set appears to be much too small). Therefore, in a cell with e.g. 20% water or bare rock, the texture value of the cell is 15 if 40% of the area is covered with coarse soils and 40% with medium soils. If the total cell area is water, the texture value is set to 0; if it is bare rock or glacier (only very few cells), the texture value equals 1. In these cases, surface runoff is assumed to be equal to total runoff. For some cells (Greenland and some islands), no texture data are provided by FAO. In this case, the texture was assumed to have a texture value of 20.

Table A2: Soil texture classes and the texture-related groundwater recharge factors

FAO soil texture class	texture value	R_{gmax} [mm/d]	f_t
coarse: sands, loamy sands and sandy loams with less than 18% clay and more than 65% sand	10	5	1
medium: sandy loams, loams, sandy clay loams, silt loams, silt, silty clay loams and clay loams with less than 35% clay and less than 65% sand; the sand fraction may be as high as 82% if a minimum of 18% clay is present	20	3	0.95
fine: clays, silty clays, sandy clays, clay loams and silty clay loams with more than 35% clay	30	1.5	0.7
rock or glacier (in 100% of cell land area)	1	0	0

Hydrogeology

A global hydrogeological map does not exist. Only for Europe and Africa, there are hydrogeological maps, which, however, use very different classifications. The Hydrogeological Map of Pan-Europe (RIVM, 1991) distinguishes among areas with good, modest, poor and no hydraulic conductivity. A hydrogeological map of Africa (UN, 1988) was derived from a geological map and only gives information on porosity but not on the more important hydraulic conductivity. A map of groundwater resources in Africa (UNDTCD, 1988) provides additional information on extensive unconfined and confined sedimentary aquifers and local, fragmented fractured aquifers.

On the global scale, only geological maps do exist. The digital Generalized Geological Map of the World (Canadian Geological Survey, 1995) provides, on a scale of 1:35 million, information on the rock type and the rock age. Rock type classes are:

1. mainly sedimentary
2. mainly volcanic
3. mixed sedimentary, volcanic and volcaniclastic
4. plutons
5. intrusive and metamorphic terranes
6. tectonic assemblages, schist belts and melanges
7. ice cap (Greenland)

From this map, the dominant rock type and rock age for the land area of each 0.5° x 0.5° cell was assigned to the respective cell.

However, this rock type classification is not very helpful for estimating where groundwater recharge is relatively high and where not, as these rock types show only a low correlation with the hydraulic conductivity of the rock. In particular, sedimentary rocks include both sands and clays, which have extremely different hydraulic conductivities. For non-sedimentary rocks, the degree of fracturing is decisive for the hydraulic conductivity, and this information is not given either. For Europe, the rock types in combination with the rock ages were compared to the Hydrogeological Map of Pan-Europe. It appears that all rock types except the type "mainly sedimentary" correlate to some degree with areas of poor or no hydraulic conductivity. The "mainly sedimentary" rock type corresponds mainly to good or modest hydraulic conductivity if the rock age is either Cenozoic or Mesozoic. Paleozoic sedimentary rocks can have any hydraulic conductivity, while Precambrian sedimentary rocks mostly have poor or no permeability. Based on this comparison to the Hydrogeological Map of Pan-Europe, only a very rough classification of hydrogeological units relevant for groundwater recharge appears to be appropriate (Table A3):

1. Cenozoic and Mesozoic sediments with high hydraulic conductivity
2. Paleozoic and Precambrian sediments with low hydraulic conductivity
3. non-sedimentary rocks with very low hydraulic conductivity

This classification was checked against the maps for Africa, and no systematic error became apparent.

High temperature and precipitation enhances weathering. Therefore, groundwater recharge is assumed to be higher in warm and humid climates. The aquifer-related recharge factors are modified based on the long-term (1961-1990) average annual temperature and precipitation in each cell.

Table A3: Hydrogeological units relevant for groundwater recharge and the aquifer-related groundwater recharge factors.

Hydrogeological units	unit value	f_a	f_a in hot and humid climate*
Cenozoic and Mesozoic sediments with high hydraulic conductivity	1	1	1
Paleozoic and Precambrian sediments with low hydraulic conductivity	2	0.7	0.8
non-sedimentary rocks with very low hydraulic conductivity	3	0.5	0.7

* average annual temperature more than 15°C and average annual precipitation more than 1000 mm (average climatic conditions 1961-1990)

Permafrost and glaciers

In the case of permafrost and glaciers, it is assumed that there is no groundwater recharge. Therefore, a data set was produced that provides the percentage of the land area of each cell that is underlain by permafrost or covered by glaciers (PG data set). The higher this percentage is, the smaller is the fraction of total runoff that recharges the groundwater.

Brown et al. (1998) provide digital data for the extent of permafrost on the northern hemisphere. Table A4 lists the five classes of permafrost extent according to Brown et al. The coverage classes were related to the average areal coverage value C_{pg} (Table A4). For North America and the Arctic islands (like Spitzbergen and Nowaja Semlja), some map units within permafrost areas are not assigned to any permafrost extent class but are classified as glaciers. However, on the rest of the map, e.g. in Norway or in the Himalayas, no information on glaciers is given, and the permafrost areas are continuous. The glacier areas in North America and the Arctic islands were assigned a value of C_{pg} = 100%.

The permafrost map was rasterized on a grid of 1/18° x 1/18°, each cell being assigned to one of the five classes in Table A4 or to the class "glacier". Then, the areal percentage of permafrost and glacier coverage within each 0.5° cell was determined as the average of the C-values of the 1/18° x 1/18° cells that are land cells on Brown et al. map.

For the southern hemisphere, no reliable maps of permafrost areas could be found, which is due to the sporadic occurrence of permafrost and the little research done. Thus, the impact of permafrost on groundwater recharge was neglected for the southern hemisphere.

Table A4: Permafrost extent classes

Permafrost extent class according to original permafrost map	C_{pg} corresponding to each class [%]	f_{pg}
continuous extent of permafrost (90-100%)	95	0.05
discontinuous extent of permafrost (50-90%)	70	0.3
sporadic extent of permafrost (10-50%)	30	0.7
isolated patches of permafrost (0-10%)	5	0.95
areas without occurrence of permafrost	0	1
glacier	100	0

In the next step, the glacier coverage for the land areas outside North America and the Arctic was included in the PG data set for WGHM. The glacier coverage was derived from the World Glacier Inventory (Hoelzle and Haeberli, 1999); in this inventory, the approximate location of the center of each glacier and its areal extent is provided. We took into account glaciers with an areal extent of at least 1 km^2, which resulted in 8998 glaciers globally (outside North America and the Arctic islands, and not considering Greenland and the Antarctic). For each 0.5° cell, the areal extents of all glaciers located within the cell were summed up. When a cell only has glaciers and no permafrost, the fraction of the glacial area with respect to the total land area of the cells is equal to the value C_{pg}. If there are both permafrost and glaciers (outside North America and the Arctic islands) within a 0.5° cell, C_{pg} is computed as

$$C_{pg} = \frac{100 * A_{gl} + C_{pg}(permafrost) * (A_{land} - A_{gl})}{A_{land}}$$

A_{gl} = sum of all glacial area in a 0.5° cell [km^2]

$C_{pg}(permafrost)$ = average C_{pg}-value due to permafrost

A_{land} = land area of 0.5° cell [km^2]

f_{pg}, the permafrost/glacier-related factor in Eq. 1, is assumed to be linearly related to C_{pg}, with f_{pg} = 1 if C_{pg} = 0% (no decrease of groundwater recharge due to glaciers and permafrost if neither of them occurs) and f_{pg} = 0 if C_{pg} = 100% (no groundwater recharge if the cell is totally covered by glaciers).